

Article

Comparison of the Transduction Capacity of AAV5 and AAV PHP.eB Serotypes in Hippocampus Astroglia

Anastasia Borodinova ^{*}, Victor Ierusalimsky and Pavel Balaban 

Laboratory of Cellular Neurobiology of Learning, Institute of Higher Nervous Activity and Neurophysiology, Russian Academy of Sciences, 117485 Moscow, Russia

^{*} Correspondence: borodinova.msu@mail.ru

Abstract: In the present study, we compared the astrocyte-transducing potential of the relatively novel engineered AAV PHP.eB serotype and the well-examined conventional AAV5 serotype. We generated the AAV-based genetic constructs with membrane-bound fluorescent markers under the control of the astroglial promoter GfaABC1D to target astrocytes *in vivo*, either via local injection into the hippocampus (AAV5, AAV PHP.eB) or via systemic injection in the retro-orbital venous sinus (AAV PHP.eB). We collected new data on the transduction properties of locally injected PHP.eB and AAV5 viruses. A morphological examination and immunostainings of mouse brain slices revealed a dose-dependent shift of cellular tropism for locally injected PHP.eB from astroglial to astroglial-neuronal as the concentration increased. When the high doses of PHP.eB viruses were administered systemically, we observed strong astrocyte transduction throughout the brain, as confirmed by the morphological examination and GFAP immunostaining. AAV5 exhibited consistent astrocytic expression in all tested concentrations. The obtained results suggest that AAV5 is more suitable for astrocyte targeting in routine stereotaxic viral injection experiments. The widely used engineered PHP.eB capsid was originally designed for the transduction of both neurons and glia. Dual cellular tropism of PHP.eB viruses, observed using different doses and different delivery protocols (local vs. systemic), suggests that the usage of AAV5 is more reliable for astrocyte labeling and that intrahippocampal injection is more suitable than systemic injection for the preferential labeling of hippocampal astroglia.



Citation: Borodinova, A.; Ierusalimsky, V.; Balaban, P. Comparison of the Transduction Capacity of AAV5 and AAV PHP.eB Serotypes in Hippocampus Astroglia. *Neuroglia* **2023**, *4*, 275–289. <https://doi.org/10.3390/neuroglia4040019>

Academic Editor: Silvia Di Angelantonio

Received: 7 August 2023

Revised: 16 October 2023

Accepted: 18 October 2023

Published: 1 November 2023



Copyright: © 2023 by the authors. Licensee MDPI, Basel, Switzerland. This article is an open access article distributed under the terms and conditions of the Creative Commons Attribution (CC BY) license (<https://creativecommons.org/licenses/by/4.0/>).

Keywords: astrocytes; adeno-associated virus; brain; transduction; central nervous system (CNS)

1. Introduction

Adeno-associated viruses (AAV) are commonly used in the lab for gene transfer and in clinical trials of gene therapies [1]. More than ten of them have been reported in humans, each possessing a tropism for specific cell types [2,3]. A new AAV variant, AAV-PHP.B, capable of penetrating the blood-brain barrier, was created several years ago [4]. Later, a novel variant, AAV-PHP.eB, has been identified and has shown greater barrier penetration than AAV-PHP.B [5]. Evidently, the penetration of the virus to deep brain areas from a single injection site is convenient in many cases (such as the treatment of neurodegenerative diseases); nevertheless, it makes the labeling of restricted (chosen) brain areas difficult. The selectivity of the viral transduction depends on a range of factors, such as the delivery method, the packaged cargo, and the capsid protein [6]. A significant body of studies on viral transduction were performed in astrocytes, due to the majority of astrocytes being found in total brain cell populations and due to the important roles the astrocytes play in brain functioning. Indeed, glial cells are several times more numerous than neurons, and astrocytes constitute the majority of the glial population [7]. The first example of the transduction of astrocytes with AAV was demonstrated by Lawlor et al. [8].

Astrocytes play many important roles in brain functioning, and a lot of attention has been paid to astrocytes recently (for a review, see [9]). Astrocytes control the homeostasis of the CNS at all levels of organization, from molecular to the whole organ. They act by

removing and catabolizing neurotransmitters and by supplying neurons with neurotransmitter precursors. They participate in embryonic and adult neurogenesis and also supply neurons with energy substrates. The range of their functions includes neurotransmitter uptake [10], the synthesis and secretion of trophic factors [11], and the regulation of synaptic density [12]. Probably the most important (and first studied) function of astrocytes is to accumulate glutamate, which is released by activated cortex cells [13]. The process of glutamate uptake was reviewed in detail by Danbolt [14]. Glutamine synthetase (GS) catalyzes the ATP-dependent condensation of ammonia and glutamate to form glutamine, thereby regulating glutamate and glutamine homeostasis [15]. Glutamine serves as the precursor molecule for glutamate synthesis. Astrocytes release glutamine into the extracellular space, which is transported to glutamatergic neurons. Most, if not all, astrocytes participate in this process, thereby protecting cells of the cortex from excitotoxic damage. Another important function of astrocytes is their participation in epilepsy development, as well as maintaining the normal brain physiology during development [16,17]. Astrocyte–neuron communication and signaling constitutes a complicated process, which has been investigated in many studies (for a review, see [18]). The recent evidence suggests that astrocytes are involved in a wide range of adaptive functions in the mammalian nervous system, including neurotransmitter uptake [10], the synthesis and secretion of trophic factors [11], aiding in the repair and regeneration of wounds [19], and the regulation of synaptic density [12].

While all astrocytes contain GS, they have glial fibrillary acidic protein immunoreactive (GFAP-ir) filaments only in a region-dependent pattern [20]. A comparative analysis of different astrocyte markers showed that astrocytes constitute a heterogeneous population, even within a given region [21,22]. The list of astrocyte functions, and consequently the list of methods for detecting astrocytes, has rapidly increased since the very first studies on glutamine-glutamate metabolism. The list of astrocyte markers includes more than twenty of the most commonly used markers, including GFAP, S100 β , and GS. For a full list of markers, please see the website of R&D Systems.

It is known that only one part of GS-ir cells also contains GFAP [21]. Evidently, one can suppose that the transduction of astrocytes with viruses under the control of the glial GfaABC1D promoter should label the entire population of GFAP-containing astrocytes. However, in fact this has never been directly studied in detail. When working with glial cells, high selectivity and efficacy rates during viral transduction are of particular interest. Earlier, we summarized the published data concerning the strategy of astrocytic targeting using different adeno-associated viruses [23]. Briefly, the effectivity of glial transduction depends on multiple parameters, including (1) the proper AAV serotype to ensure the binding of viral capsid proteins with specific receptors on the cellular membrane in a cell-type-specific manner and (2) the appropriate promoter to selectively work in the chosen population of cells. Other factors such as the AAV purification protocol, route of AAV injection, and animal age may also influence the results [24]. Within the range of conventional serotypes, AAV5 has demonstrated high astrocyte tropism and great transduction efficiency rates, and it has been repeatedly exploited in many recent studies for astrocytes transduction [1,25–34]. It was shown earlier [35] that AAV5 particles do not bind to high-affinity receptors in the brain, meaning they diffuse over larger areas. Recent advances in molecular engineering and the use of a directed evolution approach allow for the development of novel synthetic serotypes with enhanced properties, such as glial tropism, on the basis of the naturally existing AAV capsids [4,6,36–38]. A method of capsid selection to develop effectively transducing capsids to transduce the CNS after intravenous injection (CREATE) was devised in recent years [4,6]. Then, it was improved into the M-CREATE version [39]. For the modern state of the CREATE method, see [38].

Conventional AAV9 has become a very common parental serotype for the molecular engineering of different viral capsids (PHP.B, PHP.A, PHP.eB, rAAV9P1) [4,5,40], although its cell specificity depends on the experimental conditions (for a review, see [23]). Engineered capsids have been developed for the efficient targeting of particular populations

of cells, including astrocytes, although they are less well-examined than the natural AAV serotypes. The widely used engineered PHP.eB capsid was originally designed for the transduction of both neurons and glia by performing parallel selections for suitable capsid modifications [5]. By pairing this PHP.eB serotype and cell-type-specific promoters, it became possible to restrict the viral expression to a particular population of cells, e.g., astrocytes [5] or neurons [41]. Multiple studies utilized an intravenous delivery approach to characterize novel PHP.eB viral vectors, leaving the transduction potential of locally injected PHP.eB viruses unexplored [1,5,34,41–43].

In the current study, we compared the transduction capacity of 2 locally injected viruses that were made on the basis of the conventional AAV5 serotype or an engineered PHP.eB serotype to express target proteins under the control of the glial GfaABC1D promoter in hippocampal astrocytes. The GfaABC1D promoter was originally identified by Lee [44]. A morphological analysis performed in parallel revealed that the AAV5 viruses at different concentrations exhibited consistent astrocytic expression, while locally the injected PHP.eB viruses provided less reliable results for either astroglial or astroglial-neuronal tropism, depending on the concentration used. Interestingly, systemic injections of high doses of PHP.eB viruses resulted in strong astrocytic tropism, which is consistent with previously published data. The obtained results suggest that similarly to conventional AAV serotypes, the cellular tropism of engineered AAV capsids depends on the delivery method and requires careful investigation.

2. Materials and Methods

2.1. Animals

The work was carried out in 2.5–5-month-old C57Black/6 male mice (Pushchino Animal Breeding Facility (BIBC RAS), Moscow, Russia). The total number of animals used was 14. All experimental procedures were conducted in accordance with the European Communities Council Directive 2010/63/EU for animal experiments and were approved (#012 from 10.10.2014) by the Ethical Committee of the Institute of Higher Nervous Activity and Neurophysiology of RAS.

2.2. Plasmids and AAVs

For astrocytic labeling, we utilized a previously made AAV plasmid with metabotropic opsin Opto-a1AR fused to EYFP, driven by the astrocyte-specific GfaABC1D promoter [45]. For the efficient transduction of brain cells, the same payload was packaged into two different recombinant AAVs followed by iodixanol gradient ultracentrifugation and purification according to a previously published protocol [46]. To generate the recombinant AAV serotype 2/5, we used the commercially available AAV5 plasmid (Addgene, #104964). To produce the recombinant AAV serotype PHP.eB, we used the available AAV PHP.eB plasmid (Addgene, #103005). The resulting virus titer was equal to 2.93×10^{14} vg/mL for AAV2/5 GfaABC1D_opto-a1AR_EYFP and 1.13×10^{14} vg/mL for AAV PHP.eB GfaABC1D_opto-a1AR_EYFP.

2.3. Stereotaxic Viral Injection

The viral solution aliquots were stored at -70 °C and used when freshly thawed. For the intrahippocampal injections of AAV5, we used viruses at three concentrations: 2×10^9 ($n = 2$), 2×10^{10} ($n = 2$), and 5×10^{10} ($n = 3$) vg (virus genomes) per animal. The AAV PHP.eB intrahippocampal injections were made at 2×10^9 ($n = 2$), and 2×10^{10} ($n = 2$) vg per animal. The animals were anesthetized with isoflurane (3–5% in 1 L/min O₂, 1.5% maintenance) and then locally anesthetized via subcutaneous lidocaine (2%) injection. A small hole in the skull was drilled over the left hippocampus CA1 area according to the reference atlas of Franklin and Paxinos [47]. The reference coordinates of the injection site were as follows: AP, -2.2 mm; ML, $+1.7$ mm; DV, -1.6 mm. The hippocampus was chosen for AAV injection, as it is known that GFAP is specifically expressed in this structure. First, 1 μ L of viral suspension was slowly injected into the hippocampus unilaterally at a

speed of 100 nL/min through the Hamilton syringe steel needle (outer diameter 0.312 mm). Following injection, the needle was left for an additional 10 min to allow for the diffusion of the viral particles and was then slowly withdrawn. The animals were then sutured, injected with an NSAID (carprofen, 5 mg/kg), and placed in a warmed home cage for recovery. To achieve the strong expression of the genetic construct, the experiments were performed three weeks later.

2.4. Retro-Orbital Viral Injection

Recombinant AAV PHP.eB was administered intravenously via the retro-orbital sinus in 4–5-month-old mice according to the standard protocol [48,49]. The animals were anesthetized with isoflurane (3–5% in 1 L/min O₂, 1.5% maintenance) during the whole procedure. The skin around the eye was pulled back until the eye protruded slightly. A 30 G needle was positioned approximately at a 45° angle to the eye, lateral to the medial canthus, and inserted behind the globe of the eye to the sinus. Approximately 70 µL of AAV PHP.eB (10¹² vg per animal) with 0.4–10 µL of sterile Fast-Green dye (20 mg/mL) was slowly injected into the sinus unilaterally (*n* = 3). The eyelid was closed after the procedure and the animal was returned to its home cage for recovery. To achieve strong expression of the genetic construct, the experiments were performed three weeks later.

2.5. Immunohistochemistry

Three weeks after the viral injections, the animals were deeply anesthetized with a sublethal dose of chloral hydrate (400 mg/kg) injected intraperitoneally and then euthanized via transcardial perfusion with phosphate-buffered saline (PBS) and a fixative (4% paraformaldehyde in PBS). The brain was removed and placed in the fixative for an additional 24 h for further immunohistochemistry processing.

The brain was sectioned using a vibratome (Leica Biosystems, Wetzlar, Germany) into 50 µm frontal slices that were processed as floating sections. For the double labeling of the virus-stained cells, we used several antibodies: mouse monoclonal anti-gial fibrillary acidic protein (GFAP) conjugated to Cy3TM (Sigma-Aldrich, St. Louis, MO, USA, C9205, working dilution 1:400); rabbit polyclonal anti-GFAP antibody (Invitrogen, Carlsbad, CA, USA, 180063); rabbit antibody to S100β (Abcam, Cambridge, UK, ab41548, working dilution 1:100). The secondary antibodies were Alexa-594-conjugated goat anti-rabbit IgG (Molecular Probes, Eugene, OR, USA, A11012, working dilution 1:500), and Alexa-594-conjugated goat anti-mouse IgG (Molecular Probes, Eugene, OR, USA, A11005, working dilution 1:500). The preparations were examined using an AxioPlan (Carl Zeiss AG, Jena, Germany) fluorescence microscope connected to a digital camera Camedia C-4000 (Olympus, Tokyo, Japan) to acquire images and photographed with a 40× objective. Some of the sections were examined and photographed with 20× and 40× objectives using a cerna-based laser scanning confocal microscope (Thorlabs, Newton, NJ, USA).

3. Results

3.1. Detection and Characterization of Virus-Infected Cells after Local Intrahippocampal Injection of AAV5

In our study, we used a combination of AAV5 and GfaABC1D, the efficiency of which for astrocyte transduction has been reliably proven in multiple studies [27,29,30,32,50]. A morphological analysis of the brain sections showed that all transduced cells belonged to the astrocyte population and had the same spongiform shape, with a dark nucleus in the center (Figure 1a,b). The total size range (with processes) was about 50–70 µm (Figure 1b). The confocal images showed the fine structure of the transduced astrocytes (Figure 1b), which is typical for cells of this type. This distribution of the fluorescent signal was associated with predominant membrane localization of the target protein (metabotropic opsin Opto-a1AR) fused with the EYFP reporter.

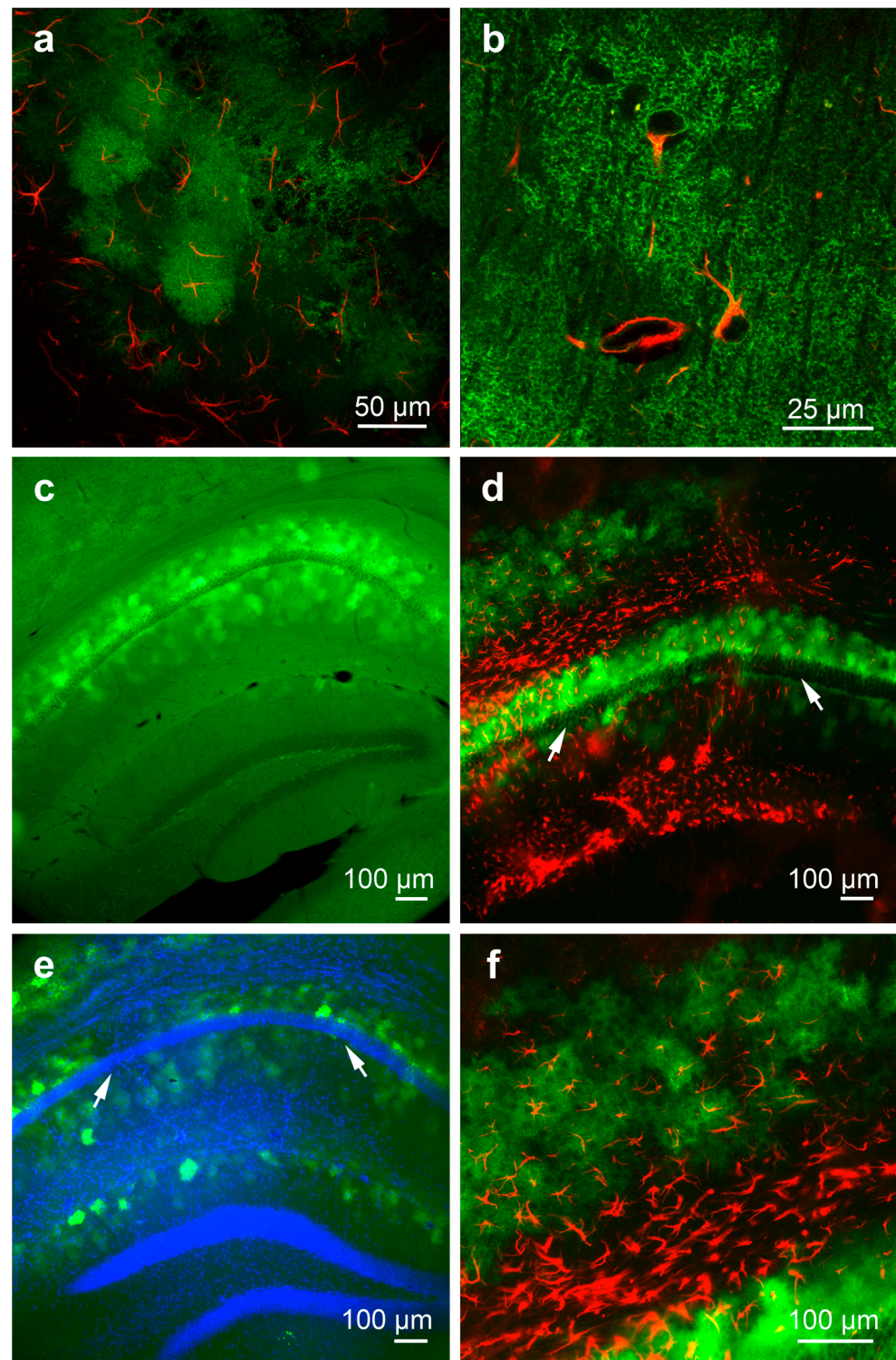


Figure 1. Morphological examination of mouse brain slices after local intrahippocampal injection of AAV5 at concentrations of 5×10^{10} (a–c) and 2×10^{10} (d–f) vg per animal. (a) Transduced cells in CA1 area (red—anti-GFAP staining). (b) High-resolution confocal image of several transduced astroglial cells (red—anti-GFAP staining). (c–e) Total view of transduced cells in the hippocampus. Virus staining combined with anti-GFAP staining (red) (d) and with DAPI (blue) (e). (d,e) The *stratum pyramidale* is marked by arrows. (f) Detailed image of (d) at higher magnification. Scale bar: 50 μm (a), 25 μm (b), 100 μm (c–f).

We tested the AAV5 at three concentrations (2×10^9 , 2×10^{10} , and 5×10^{10} vg per animal) and observed similar patterns of staining (compare Figure 1c,d). The morphological examination of the frontal brain slices revealed an irregular distribution of transduced astrocytes in the hippocampal area, consisting of one to three clusters. First, the main population was located in the *stratum radiatum* and *stratum oriens*, close to the *stratum pyramidale* layer (Figure 1c–e, arrows). The second one was located in the depth of the cortex at a distance of 400–500 μm from the hippocampus (Figure 1d,e). In some preparations, a third population of transduced astrocytes was found in the *stratum moleculare* (Figure 1e). The total length of the virus-infected area of the hippocampus was about 1500–2000 μm in the frontal plane for AAV5 (2×10^{10} vg per animal) and the stained cells formed a structure reminiscent of a dome.

As the genetic construct with the fluorescent reporter was synthesized under the control of the astrocyte-specific GfaABC1D promoter, we expected the transduced cells to be the GFAP-positive astrocyte population. To check the correct targeting of astrocytes by AAV5 viruses, we immunohistochemically stained the brain slices with an antibody to the astrocytic marker GFAP and analyzed the co-localization of fluorescent signals from transduced and GFAP(+) cells. Although both types of cells were mainly present in the hippocampus area, we found that AAV5 targeted only a fraction of the GFAP(+) astrocyte population. There were more GFAP-immunopositive cells than virus-infected cells (Figures 1f and 2c); however, all transduced cells were also GFAP-immunopositive (Figure 1f). We counted the total number of GFAP(+) cells and transduced cells in 8 sections from 2 animals injected with the AAV5 virus at a concentration of 2×10^{10} vg per animal. The mean percentage of virus-transduced cells relative to the total number of GFAP(+) cells was $31 \pm 5\%$ (Figure 3a).

Interestingly, the population of GFAP(+) cells was more numerous in areas where the number of virus-infected cells was small (Figure 1d,f). The GFAP-immunoreactive astrocytes looked like nuclei with several thick processes and were located mainly in the *stratum lacunosum-moleculare* (Figure 2a,b). Thus, the main distributions of transduced and GFAP-immunoreactive cells were partially different. At the injection site, both in sham-operated mice and in mice injected with AAV5, we observed an excessive number of GFAP(+) astrocytes, which indicated gliosis (compare Figure 2a,b).

In an additional set of experiments, we sought to confirm the correct targeting of astrocytes by AAV5 viruses using the astrocytic marker S100 β , which usually identifies a wide population of astrocytes [20,51]. Antibodies against S100 β visualize the nuclei of astrocytes and partially the cytoplasm, while the processes of these cells are only lightly stained [52]. The immunohistochemical staining revealed a widespread population of S100 β (+) cells located more or less regularly in all areas of the brain, including the hippocampus (Figure 2d). The density and total number of S100 β (+) cells were much greater than the number of transduced cells. We found only a partial overlap between S100 β (+) astrocytes and virus-infected cells (Figure 2e). We counted the total number of S100 β (+) cells and transduced cells in 9 sections from 2 animals injected with AAV5 virus at a concentration of 2×10^{10} vg per animal. The mean percentage of virus-transduced cells relative to the total number of S100 β (+) cells was $12 \pm 4\%$ (Figure 3b).

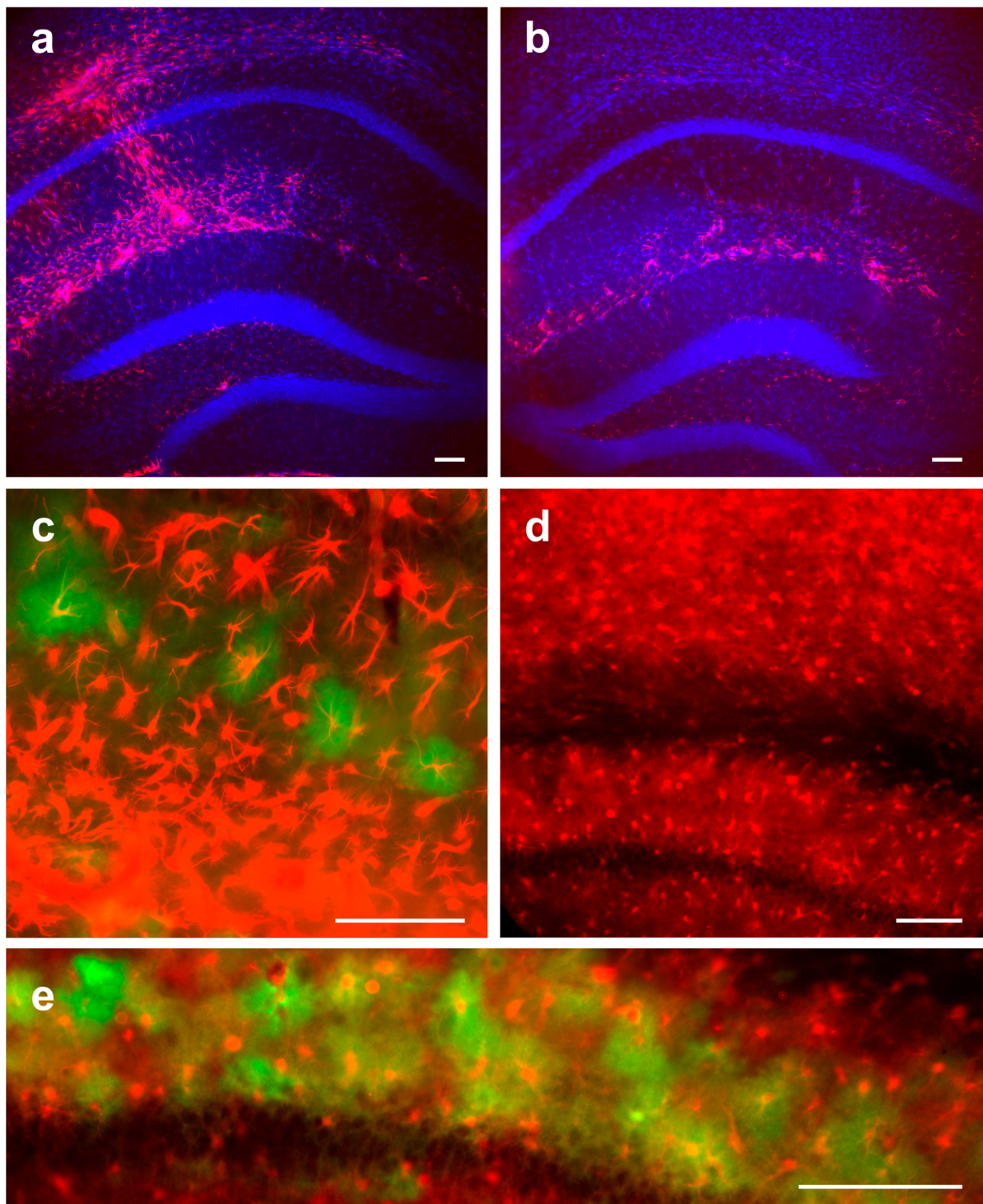


Figure 2. Immunohistochemical examination of mouse brain slices after local intrahippocampal injection of AAV5 at a concentration of 2×10^9 vg per animal. (a,b) Sections of left and right brain hemispheres stained by anti-GFAP antibody (red) and DAPI (blue). Note the difference in (a) GFAP-immunopositive cells located both in the hippocampal area and the area above it, reflecting the injection site. (b) The intact hemisphere demonstrates GFAP-immunopositive cells only inside the hippocampal area. (c) Superposition of transduced cells (green) and GFAP-immunopositive cells (red). (d) S100 β -immunopositive cells (red). (e) Partial co-localization between S100 β -immunoreactive (red) and virus-infected (green) cells. Scale bar: 100 μ m.

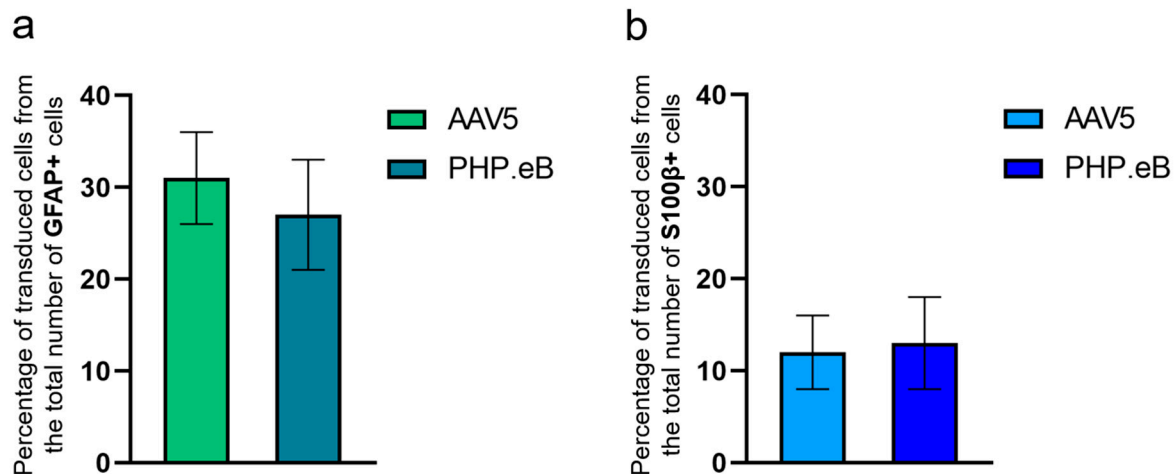


Figure 3. Percentage of virus-transduced cells from the total number of hippocampal astrocytes stained with GFAP (a) or S100β (b) glial markers.

3.2. Detection and Characterization of Virus-Infected Cells after Local Intrahippocampal Injection of AAV PHP.eB

To compare AAV PHP.eB and AAV5, we injected the viruses into the same brain area using the same protocol. The previous studies had mainly focused on the intravenous delivery of AAV PHP.eB viruses [1,5,34,41–43], leaving unexplored the transduction potential of locally injected PHP.eB viruses. In this study, we performed local injections of AAV PHP.eB viruses into the hippocampus at two concentrations, 2×10^9 and 2×10^{10} vg per animal, and found drastic changes in the patterns of staining as the virus concentration increased. At a concentration of 2×10^9 , the virus exclusively targeted astrocytes (Figure 4a), the distribution of which coincided with the distribution of AAV5-transduced cells and also included GFAP(+) astrocytes. Surprisingly, at a concentration of 2×10^{10} , we observed not only GFAP(+) astrocytes infected with the virus but also to a lesser extent hippocampal neurons (Figure 4b,c). At this viral concentration, the transduced cells were located more or less evenly in the hippocampus (Figure 4b).

The immunohistochemical staining of brain slices with an antibody to the astrocytic marker GFAP revealed that the PHP.eB viruses targeted only a small fraction of the GFAP(+) astrocyte population. There were more GFAP-immunopositive cells than virus-infected cells, although virtually all transduced cells were GFAP-immunopositive (Figure 4b,c). We counted the total number of GFAP(+) cells and transduced cells in 11 sections from 2 animals injected with the PHP.eB virus at a concentration of 2×10^9 vg per animal. The mean percentage of virus-transduced cells relative to the total number of GFAP(+) cells was $27 \pm 6\%$ (Figure 3a).

We also immunohistochemically stained brain slices with an antibody to another astrocytic marker S100β and identified a widespread population of S100β(+) cells. As it was noted earlier in experiments with AAV5, the total number of S100β(+) cells was much greater than the number of transduced cells. We found only partial overlap between S100β(+) astrocytes and virus-infected cells. We counted the total number of S100β(+) cells and transduced cells in 9 sections from 2 animals injected with the PHP.eB virus at a concentration of 2×10^9 vg per animal. The mean percentage of virus-transduced cells relative to the total number of S100β(+) cells was $13 \pm 5\%$ (Figure 3b).

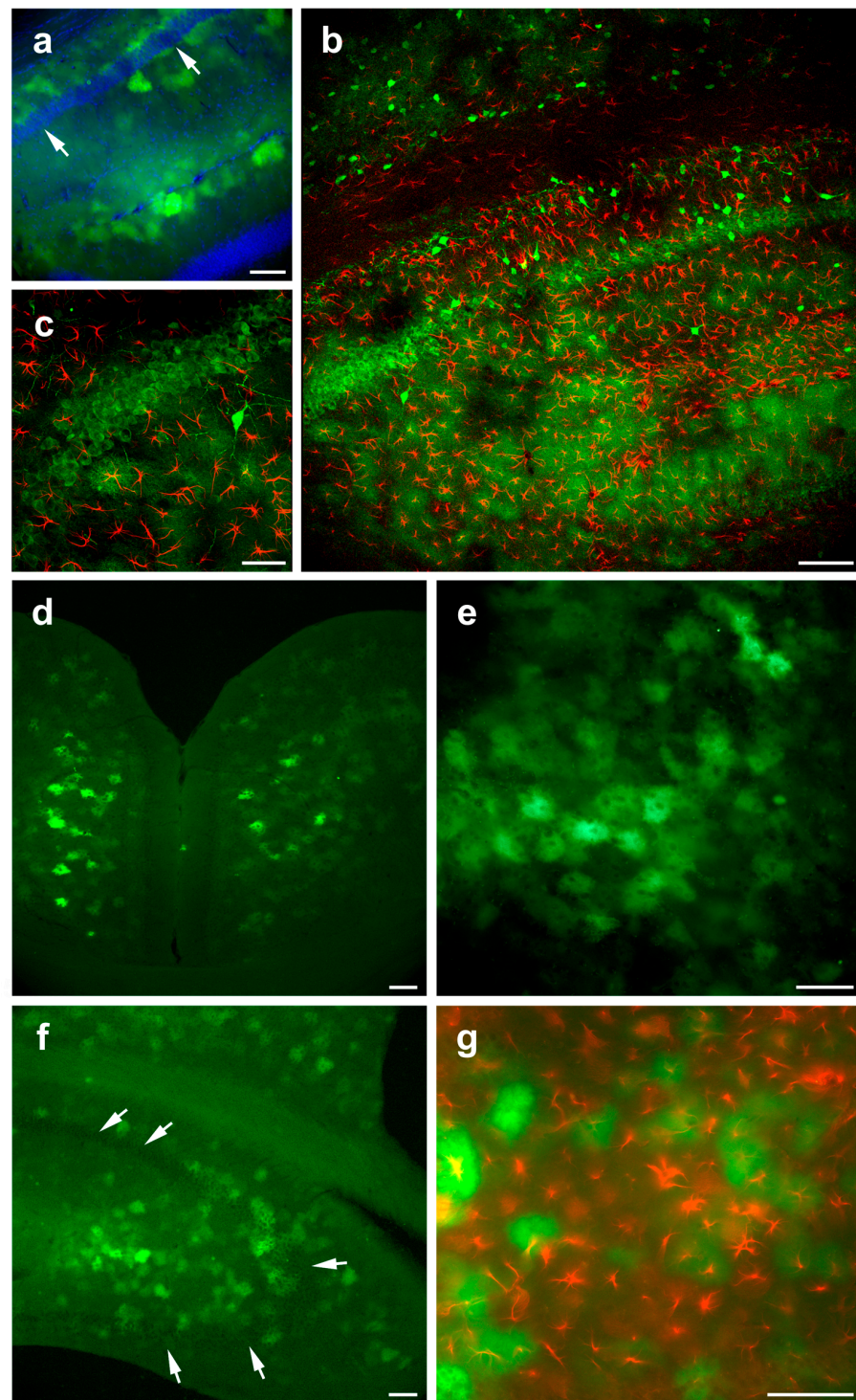


Figure 4. Morphological examination of mouse brain slices after local intrahippocampal injection (a–c) and systemic, retro-orbital injection (d–g) of AAV PHP.eB. Viral concentrations of 2×10^9 (a), 2×10^{10} (b,c), and 10^{12} (d–g) vg per animal. (a) The reaction is limited to astrocytes (blue staining is DAPI, *stratum pyramidale* is matched by arrows), while (b,c) neurons in the *stratum pyramidale* are stained as well (red—anti-GFAP staining). (c) Detailed image of (b) at higher magnification. Systemic injection of AAV PHP.eB revealed transduced cells in different brain areas: (d) retrosplenial cortex; (e) typical group of virus-infected cells in the somatosensory cortex; (f) virus-infected cells in the ventral hippocampus (matched by arrows); (g) superposition of virus-stained cells (green) and GFAP-immunopositive cells (red) in somatosensory cortex. Scale bar: 100 μm .

3.3. Detection and Characterization of Virus-Infected Cells after Systemic Retro-Orbital Injection of AAV PHP.eB

Numerous studies show that AAV PHP.eB can be successfully applied to transduce glial cells when injected systemically in the retro-orbital venous sinus of adult mice [5,34,39,48]. To exclude specific experimental conditions that may affect viral properties, such as cellular tropism [23,44], we administered high doses (10^{12} vg per animal) of AAV PHP.eB systemically as previously described [41,48,49]. We found virus-infected cells (green) in most areas of the brain, including the retrosplenial (Figure 4d) and somatosensory (Figure 4e) cortices, as well as in many subcortical structures. The cells were unevenly distributed throughout the cortical layers. A visual analysis showed that the total number of stained cells was several hundred cells on a 50- μ m section, i.e., much more than the number of transduced cells after an intrahippocampal injection of PHP.eB. Figure 4d shows a typical group of stained cortical cells. The patterns of stained cells were variable, with big and small groups of cells and single cells. The virus-transduced cells were also found in the hippocampus region, and their number in this area was relatively small (80–120 cells per 50- μ m section). The types of distribution in the hippocampus differed from the distribution observed after local injection, with only a diffuse group found in the ventral hippocampus (Figure 4f) but not layered populations of transduced cells. The immunohistochemical analysis revealed that most of the virus-infected cells were GFAP-positive (Figure 4g). Based on the morphological analysis, it can be concluded that the systemic delivery of the viral suspension to the brain resulted in a transduction pattern of glial cells of approximately the same size and shape, similar to the pattern observed after the local injection of AAV PHP.eB at a concentration of 2×10^9 vg per animal.

4. Discussion

Given the important role of astrocytes in the normal brain physiology and pathology, considerable efforts have been focused on selectively targeting astrocytes and modulating their functions using various AAV vectors. The purpose of this study was a parallel comparison of the astrocyte-transducing potential of the relatively novel AAV PHP.eB and widely used conventional AAV5.

It is well known that astrocytes (e.g., S100 β -immunopositive cells) occupy the entire hippocampal area. We found that the distribution patterns of the transduced cells differed significantly depending on the AAV administration protocol. After local (intrahippocampal) injections of AAV5 and AAV PHP.eB, we observed transduced cells over a broad hippocampus area, grouped into narrow layers located in the *stratum oriens* and *stratum radiatum* areas and sometimes in the *stratum moleculare* (Figures 1 and 4). The transduction area covered the entire depth of the hippocampus and reached a length of about 1.5 mm. The transduction potential of AAV5 was reasonably limited to astrocytes at all three concentrations tested (2×10^9 , 2×10^{10} , 5×10^{10} vg per animal). However, following the local injection of AAV PHP.eB, the specificity of the viral transduction changed from exclusively astroglial (2×10^9) to mixed astroglial—neuronal (2×10^{10}), with a large number of transduced neurons in the *stratum pyramidale* (Figure 4a–c).

In contrast, after the systemic (retro-orbital) injection of AAV PHP.eB, the transduced cells were diffusely distributed in all areas of the hippocampus and in the cerebral cortex (Figure 4d–f), as well as beyond them, which is consistent with previously published data on AAV PHP.eB under the control of a neuron-specific promoter [1]. The transduction potential of the systemically injected AAV PHP.eB (10^{12} vg per animal) was limited to astrocytes in various brain regions, which is consistent with the previously published data.

Some experimental data suggest that the cellular tropism of certain AAV serotypes may depend on the viral delivery strategy. For example, transgene expression driven by the ubiquitous CB promoter was observed predominantly in astrocytes when AAV9 vectors were administered systemically and in neurons when the same viruses were injected locally [53]. Several studies suggest that AAV PHP.eB has similar properties to the parental AAV9 capsid and demonstrates similar cell-specific targeting when injected systemically

into the retro-orbital venous sinus (the glial promoter GfaABC1D was used [5]) or locally injected into cerebral ventricles bypassing the blood-brain barrier (the ubiquitous CAG promoter was used) [54]. Our results complement this idea and show either astrocytic or mixed astrocytic-neuronal transduction patterns for the same AAV PHP.eB virus, depending on the viral delivery protocol (Figure 4). Unlike previous studies, we observed transgene expression in neurons using genetic constructs controlled by the glial promoter GfaABC1D (Figure 4b,c), which has rarely been reported in the literature [30,55,56]. In a comprehensive study of GFAP promoter elements, Lee and colleagues did not provide any reasonable background for this unusual transgene expression driven by the GfaABC1D promoter [44]. Immunostaining for different cellular markers in the peripheral and central nervous system demonstrated little or no GfaABC1D-driven expression in neurons (NeuN), microglia (Iba1), oligodendrocytes (CNPase), and NG2 glial cells (NG2) [30,31,34,50]. Nevertheless, it was clearly demonstrated by Taschenberger et al. [56] that the GfaABC1D promoter can be leaky and insufficient for specific transgene expression in astrocytes. The dual cellular tropism of PHP.eB viruses observed using different doses and different delivery protocols (local vs. systemic) resembles the properties of the parental capsid AAV9 and requires careful investigation of transgene expression in each case.

The GfaABC1D-driven expression of membrane-bound fluorescent proteins distributed across the membrane allowed us to trace the fine structure of the infected cells and uniquely identify them as astrocytes (Figure 1b), with the morphology aligning with that described earlier in numerous studies [15,23,27,29,32,45,46,50,57,58].

To check the correct targeting of astrocytes by AAV5 and PHP.eB, we immunostained brain slices for the classical astroglial markers GFAP and S100 β to define subpopulations of astrocytes targeted by the tested AAVs. We found that both virus serotypes, regardless of the concentration used, infected only a part of the astrocyte population, as was revealed by anti-GFAP and anti-S100 β staining. Anti-GFAP staining usually reveals the astrocytes' somata and main processes [52]. In a detailed study of astrocyte morphology by Bushong et al. [57], it was established that GFAP marks out only approximately 15% of the total astrocyte volume. In contrast, viral transduction causes the expression of the fluorescent reporter protein in fine processes, as has been revealed in numerous studies [15,29–31,50,58]. In our experiments, the GfaABC1D-driven expression of a membrane-bound fluorescent reporter allowed us to detect fine processes of an astrocyte, shaped in a spongiform structure, while somata and thick processes were detected via staining against GFAP (Figure 1a,b,d,f). This is consistent with previously published studies, demonstrating the strong specificity of the GfaABC1D promoter towards astrocytes [8,27,29–32,34,50,59]. As expected, almost all virus-infected cells with the astrocyte morphology were GFAP-positive, although their number was about 30% of the total population of GFAP-positive hippocampal astrocytes.

It is a well-known fact that astroglia represent heterogeneous populations of cells that differ in their morphology and in the expressed molecular markers [51,60–62]. Some markers, such as GFAP, show region-specific immunoreactivity, which is most pronounced in the hippocampus [51], although GFAP staining reveals only about 60% of the total number of GS-positive cells [21]. In our work, AAV labeled about 30% of the GFAP(+) cells. This suggests that viral transduction, even after local injection of the virus, targets only a small population of astrocytes.

Another marker, S100 β , used in our work, displayed a more uniform distribution inside the brain (Figure 2d); therefore, S100 β staining allows the detection of much broader populations of astrocytes [20,51]. Nagai and colleagues showed that AAV5 vectors driven by the GfaABC1D promoter provide almost 93% overlap of transduced and S100 β -positive astrocytes in the striatum [34]. In our work, almost all infected cells were also S100 β -positive, although they accounted for only a small part of the entire S100(+) population (Figure 2e). Taken together, our data indicate that this method of viral transduction allows certain subpopulations of astrocytes to be infected but is not ideal for targeting the entire population of hippocampal astrocytes, and other approaches can be considered [34].

In summary, our study provides a comparison of the conventional AAV5 and engineered AAV PHP.eB, giving new information about their ability to transduce astrocytes in the hippocampus. A morphological examination and the immunostaining of brain slices for various astroglial markers revealed distinct transduction patterns for the tested AAVs injected locally into the hippocampus. AAV5 exhibited consistent astrocyte transduction at all tested concentrations, while PHP.eB demonstrated either glial or mixed glial-neuronal tropism, depending on the concentration used. Therefore, the obtained results suggest that AAV5 is more suitable for targeting astrocytes in routine stereotaxic viral injection experiments. Given the ability of AAV PHP.eB to cross the blood-brain barrier, we administered the PHP.eB viruses systemically and demonstrated strong astrocyte transduction throughout the brain, which corresponds to the previously published data. Therefore, AAV PHP.eB requires a careful investigation of its expression in each case, although under certain conditions AAV PHP.eB viruses can also allow the efficient and selective targeting of astrocytes.

5. Conclusions

The data suggest that AAV5 is more reliable for labeling astrocytes than AAV PHP.eB and that intrahippocampal injection is more suitable for the preferred labeling of hippocampal astrocytes than systemic injection.

Author Contributions: A.B., conceptualization, investigation, writing—original draft. V.I., investigation, visualization, formal analysis, writing—original draft. P.B., supervision, writing—reviewing and editing, funding acquisition. All authors have read and agreed to the published version of the manuscript.

Funding: This research was supported by a grant of Russian Science Foundation, #20-15-00408.

Institutional Review Board Statement: The study was conducted in accordance with the European Communities Council Directive 2010/63/EU for animal experiments and was approved (#012 from 10.10.2014) by the Ethics Committee of the Institute of Higher Nervous Activity and Neurophysiology of RAS.

Informed Consent Statement: Not applicable.

Data Availability Statement: The data that support the findings of this study are available from the corresponding author, A. Borodinova, upon reasonable request.

Acknowledgments: We thank M. Roshchin for his help with the intrahippocampal stereotaxic viral injections. The authors are grateful to A. Lazutkin, A. Revishchin, and G. Pavlova for the kind gift of antibodies. The authors are grateful to A. Malyshev for his help in obtaining confocal images.

Conflicts of Interest: The authors declare no conflict of interest.

References

1. Xie, B.-S.; Wang, X.; Pan, Y.-H.; Jiang, G.; Feng, J.-F.; Lin, Y. Apolipoprotein E, low-density lipoprotein receptor, and immune cells control blood-brain barrier penetration by AAV-PHP.eB in mice. *Theranostics* **2021**, *11*, 1177–1191. [[CrossRef](#)]
2. Daya, S.; Berns, K.I. Gene therapy using adeno-associated virus vectors. *Clin. Microbiol. Rev.* **2008**, *21*, 583–593. [[CrossRef](#)]
3. Colella, P.; Ronzitti, G.; Mingozzi, F. Emerging issues in AAV-Mediated in vivo gene therapy. *Mol. Ther.-Methods Clin. Dev.* **2018**, *8*, 87–104. [[CrossRef](#)]
4. Deverman, B.E.; Pravdo, P.L.; Simpson, B.P.; Kumar, S.R.; Chan, K.Y.; Banerjee, A.; Wu, W.-L.; Yang, B.; Huber, N.; Pasca, S.P.; et al. Cre-dependent selection yields AAV variants for widespread gene transfer to the adult brain. *Nat. Biotechnol.* **2016**, *34*, 204–209. [[CrossRef](#)]
5. Chan, K.Y.; Jang, M.J.; Yoo, B.B.; Greenbaum, A.; Ravi, N.; Wu, W.-L.; Sánchez-Guardado, L.; Lois, C.; Mazmanian, S.K.; Deverman, B.E.; et al. Engineered AAVs for efficient noninvasive gene delivery to the central and peripheral nervous systems. *Nat. Neurosci.* **2017**, *20*, 1172–1179. [[CrossRef](#)]
6. Bedbrook, C.N.; Deverman, B.E.; Gradinaru, V. Viral strategies for targeting the central and peripheral nervous systems. *Annu. Rev. Neurosci.* **2018**, *41*, 323–348. [[CrossRef](#)]
7. Kimelberg, H.K.; Norenberg, M.D. Astrocytes. *Sci. Am.* **1989**, *260*, 66–76. [[CrossRef](#)]
8. Lawlor, P.A.; Bland, R.J.; Mouravlev, A.; Young, D.; During, M.J. Efficient gene delivery and selective transduction of glial cells in the mammalian brain by AAV serotypes isolated from nonhuman primates. *Mol. Ther.* **2009**, *17*, 1692–1702. [[CrossRef](#)]

9. Verkhatsky, A.; Nedergaard, M. Physiology of astroglia. *Physiol. Rev.* **2018**, *98*, 239–389. [[CrossRef](#)]
10. Diamond, J.S.; Jahr, C.E. Transporters buffer synaptically released glutamate on a submillisecond time scale. *J. Neurosci.* **1997**, *17*, 4672–4687. [[CrossRef](#)]
11. Liesi, P.; Silver, J. Is astrocyte laminin involved in axon guidance in the mammalian CNS? *Dev. Biol.* **1988**, *130*, 774–785. [[CrossRef](#)]
12. Meshul, C.K.; Seil, F.J.; Herndon, R.M. Astrocytes play a role in regulation of synaptic density. *Brain Res.* **1987**, *402*, 139–145. [[CrossRef](#)]
13. Norenberg, M.D.; Martinez-Hernandez, A. Fine structural localization of glutamine synthetase in astrocytes of rat brain. *Brain Res.* **1979**, *161*, 303–310. [[CrossRef](#)]
14. Danbolt, N.C. Glutamate uptake. *Prog. Neurobiol.* **2001**, *65*, 1–105. [[CrossRef](#)]
15. Bernstein, H.-G.; Bannier, J.; Meyer-Lotz, G.; Steiner, J.; Keilhoff, G.; Dobrowolny, H.; Walter, M.; Bogerts, B. Distribution of immunoreactive glutamine synthetase in the adult human and mouse brain. Qualitative and quantitative observations with special emphasis on extra-astroglial protein localization. *J. Chem. Neuroanat.* **2014**, *61–62*, 33–50. [[CrossRef](#)]
16. Wu, Y.; Zhang, A.-Q.; Yew, D.T. Age related changes of various markers of astrocytes in senescence-accelerated mice hippocampus. *Neurochem. Int.* **2005**, *46*, 565–574. [[CrossRef](#)]
17. Eid, T.; Lee, T.W.; Patrylo, P.; Zaveri, H.P. Astrocytes and glutamine synthetase in epileptogenesis. *J. Neurosci. Res.* **2018**, *97*, 1345–1362. [[CrossRef](#)]
18. Haydon, P.G.; Carmignoto, G. Astrocyte control of synaptic transmission and neurovascular coupling. *Physiol. Rev.* **2006**, *86*, 1009–1031. [[CrossRef](#)]
19. Rudge, J.S.; Smith, G.M.; Silver, J. An in vitro model of wound healing in the CNS: Analysis of cell reaction and interaction at different ages. *Exp. Neurol.* **1989**, *103*, 1–16. [[CrossRef](#)]
20. Anlauf, E.; Derouiche, A. Glutamine synthetase as an astrocytic marker: Its cell type and vesicle localization. *Front. Endocrinol.* **2013**, *4*, 144. [[CrossRef](#)]
21. Walz, W.; Lang, M.K. Immunocytochemical evidence for a distinct GFAP-negative subpopulation of astrocytes in the adult rat hippocampus. *Neurosci. Lett.* **1998**, *257*, 127–130. [[CrossRef](#)]
22. Zhang, Y.; Barres, B.A. Astrocyte heterogeneity: An underappreciated topic in neurobiology. *Curr. Opin. Neurobiol.* **2010**, *20*, 588–594. [[CrossRef](#)]
23. Borodinova, A.A.; Balaban, P.M.; Bezprozvanny, I.B.; Salmina, A.B.; Vlasova, O.L. Genetic constructs for the control of astrocytes' activity. *Cells* **2021**, *10*, 1600. [[CrossRef](#)]
24. Klein, R.L.; Dayton, R.D.; Tatom, J.B.; Henderson, K.M.; Henning, P.P. AAV8, 9, Rh10, Rh43 vector gene transfer in the rat brain: Effects of serotype, promoter and purification method. *Mol. Ther.* **2008**, *16*, 89–96. [[CrossRef](#)] [[PubMed](#)]
25. Ortinski, P.I.; Dong, J.; Mungenast, A.; Yue, C.; Takano, H.; Watson, D.J.; Haydon, P.G.; Coulter, D.A. Selective induction of astrocytic gliosis generates deficits in neuronal inhibition. *Nat. Neurosci.* **2010**, *13*, 584–591. [[CrossRef](#)] [[PubMed](#)]
26. Chakrabarty, P.; Rosario, A.; Cruz, P.; Siemienski, Z.; Ceballos-Diaz, C.; Crosby, K.; Jansen, K.; Borchelt, D.R.; Kim, J.-Y.; Jankowsky, J.L.; et al. Capsid serotype and timing of injection determines AAV transduction in the neonatal mice brain. *PLoS ONE* **2013**, *8*, e67680. [[CrossRef](#)]
27. Shigetomi, E.; Bushong, E.A.; Hausteiner, M.D.; Tong, X.; Jackson-Weaver, O.; Kracun, S.; Xu, J.; Sofroniew, M.V.; Ellisman, M.H.; Khakh, B.S. Imaging calcium microdomains within entire astrocyte territories and endfeet with GCaMPs expressed using adeno-associated viruses. *J. Gen. Physiol.* **2013**, *141*, 633–647. [[CrossRef](#)]
28. Chai, H.; Diaz-Castro, B.; Shigetomi, E.; Monte, E.; Octeau, J.C.; Yu, X.; Cohn, W.; Rajendran, P.S.; Vondriska, T.M.; Whitelegge, J.P.; et al. Neural circuit-specialized astrocytes: Transcriptomic, proteomic, morphological, and functional evidence. *Neuron* **2017**, *95*, 531–549.e9. [[CrossRef](#)]
29. Adamsky, A.; Kol, A.; Kreisel, T.; Doron, A.; Ozeri-Engelhard, N.; Melcer, T.; Refaeli, R.; Horn, H.; Regev, L.; Groysman, M.; et al. Astrocytic activation generates de novo neuronal potentiation and memory enhancement. *Cell* **2018**, *174*, 59–71.e14. [[CrossRef](#)]
30. Griffin, J.M.; Fackelmeier, B.; Fong, D.M.; Mouravlev, A.; Young, D.; O'carroll, S.J. Astrocyte-selective AAV gene therapy through the endogenous GFAP promoter results in robust transduction in the rat spinal cord following injury. *Gene Ther.* **2019**, *26*, 198–210. [[CrossRef](#)]
31. Li, Y.; Li, L.; Wu, J.; Zhu, Z.; Feng, X.; Qin, L.; Zhu, Y.; Sun, L.; Liu, Y.; Qiu, Z.; et al. Activation of astrocytes in hippocampus decreases fear memory through adenosine A1 receptors. *eLife* **2020**, *9*, e57155. [[CrossRef](#)] [[PubMed](#)]
32. Testen, A.; Kim, R.; Reissner, K.J. High-resolution three-dimensional imaging of individual astrocytes using confocal microscopy. *Curr. Protoc. Neurosci.* **2020**, *91*, e92. [[CrossRef](#)] [[PubMed](#)]
33. Yu, X.; Nagai, J.; Marti-Solano, M.; Soto, J.S.; Coppola, G.; Babu, M.M.; Khakh, B.S. Context-specific striatal astrocyte molecular responses are phenotypically exploitable. *Neuron* **2020**, *108*, 1146–1162.e10. [[CrossRef](#)] [[PubMed](#)]
34. Nagai, J.; Bellafard, A.; Qu, Z.; Yu, X.; Ollivier, M.; Gangwani, M.R.; Diaz-Castro, B.; Coppola, G.; Schumacher, S.M.; Golshani, P.; et al. Specific and behaviorally consequential astrocyte Gq GPCR signaling attenuation in vivo with i β ARK. *Neuron* **2021**, *109*, 2256–2274.e9. [[CrossRef](#)] [[PubMed](#)]
35. Blits, B.; Derks, S.; Twisk, J.; Ehlert, E.; Prins, J.; Verhaagen, J. Adeno-associated viral vector (AAV)-mediated gene transfer in the red nucleus of the adult rat brain: Comparative analysis of the transduction properties of seven AAV serotypes and lentiviral vectors. *J. Neurosci. Methods* **2010**, *185*, 257–263. [[CrossRef](#)] [[PubMed](#)]

36. Koerber, J.T.; Klimczak, R.; Jang, J.-H.; Dalkara, D.; Flannery, J.G.; Schaffer, D.V. Molecular evolution of adeno-associated virus for enhanced glial gene delivery. *Mol. Ther.* **2009**, *17*, 2088–2095. [[CrossRef](#)]
37. O'carroll, S.J.; Cook, W.H.; Young, D. AAV Targeting of glial cell types in the central and peripheral nervous system and relevance to human gene therapy. *Front. Mol. Neurosci.* **2021**, *13*, 618020. [[CrossRef](#)]
38. Challis, R.C.; Kumar, S.R.; Chen, X.; Goertsen, D.; Coughlin, G.M.; Hori, A.M.; Chuapoco, M.R.; Otis, T.S.; Miles, T.F.; Gradinaru, V. Adeno-associated virus toolkit to target diverse brain cells. *Annu. Rev. Neurosci.* **2022**, *45*, 447–469. [[CrossRef](#)]
39. Kumar, S.R.; Miles, T.F.; Chen, X.; Brown, D.; Dobрева, T.; Huang, Q.; Ding, X.; Luo, Y.; Einarsson, P.H.; Greenbaum, A.; et al. Multiplexed Cre-dependent selection yields systemic AAVs for targeting distinct brain cell types. *Nat. Methods* **2020**, *17*, 541–550. [[CrossRef](#)]
40. Bauer, A.; Puglisi, M.; Nagl, D.; Schick, J.A.; Werner, T.; Klingl, A.; El Andari, J.; Hornung, V.; Kessler, H.; Götz, M.; et al. Molecular signature of astrocytes for gene delivery by the synthetic adeno-associated viral vector rAAV9P1. *Adv. Sci.* **2022**, *9*, e2104979. [[CrossRef](#)]
41. Radhiyanti, P.T.; Konno, A.; Matsuzaki, Y.; Hirai, H. Comparative study of neuron-specific promoters in mouse brain transduced by intravenously administered AAV-PHP.eB. *Neurosci. Lett.* **2021**, *756*, 135956. [[CrossRef](#)]
42. Huang, Q.; Chan, K.Y.; Tobey, I.G.; Chan, Y.A.; Poterba, T.; Boutros, C.L.; Balazs, A.B.; Daneman, R.; Bloom, J.M.; Seed, C.; et al. Delivering genes across the blood-brain barrier: LY6A, a novel cellular receptor for AAV-PHP.B capsids. *PLoS ONE* **2019**, *14*, e0225206. [[CrossRef](#)]
43. Brown, D.; Altermatt, M.; Dobрева, T.; Chen, S.; Wang, A.; Thomson, M.; Gradinaru, V. Deep parallel characterization of AAV tropism and AAV-mediated transcriptional changes via single-cell RNA sequencing. *Front. Immunol.* **2021**, *12*, 730825. [[CrossRef](#)] [[PubMed](#)]
44. Lee, Y.; Messing, A.; Su, M.; Brenner, M. GFAP promoter elements required for region-specific and astrocyte-specific expression. *Glia* **2008**, *56*, 481–493. [[CrossRef](#)] [[PubMed](#)]
45. Gerasimov, E.; Erofeev, A.; Borodinova, A.; Bolshakova, A.; Balaban, P.; Bezprozvanny, I.; Vlasova, O.L. Optogenetic activation of astrocytes—Effects on neuronal network function. *Int. J. Mol. Sci.* **2021**, *22*, 9613. [[CrossRef](#)]
46. Maltsev, A.; Roshchin, M.; Bezprozvanny, I.; Smirnov, I.; Vlasova, O.; Balaban, P.; Borodinova, A. Bidirectional regulation by “star forces”: Ionotropic astrocyte’s optical stimulation suppresses synaptic plasticity, metabotropic one strikes back. *Hippocampus* **2023**, *33*, 18–36. [[CrossRef](#)] [[PubMed](#)]
47. Franklin, K.B.J.; Paxinos, G. *The Mouse Brain in Stereotaxic Coordinates*; Academic Press: San Diego, CA, USA, 2007.
48. Challis, R.C.; Kumar, S.R.; Chan, K.Y.; Challis, C.; Beadle, K.; Jang, M.J.; Kim, H.M.; Rajendran, P.S.; Tompkins, J.D.; Shivkumar, K.; et al. Systemic AAV vectors for widespread and targeted gene delivery in rodents. *Nat. Protoc.* **2019**, *14*, 379–414. [[CrossRef](#)]
49. Yardeni, T.; Eckhaus, M.; Morris, H.D.; Huizing, M.; Hoogstraten-Miller, S. Retro-orbital injections in mice. *Lab Anim.* **2011**, *40*, 155–160. [[CrossRef](#)]
50. Xie, Y.; Wang, T.; Sun, G.; Ding, S. Specific disruption of astrocytic Ca²⁺ signaling pathway in vivo by adeno-associated viral transduction. *Neuroscience* **2010**, *170*, 992–1003. [[CrossRef](#)]
51. Zhang, Z.; Ma, Z.; Zou, W.; Guo, H.; Liu, M.; Ma, Y.; Zhang, L. The appropriate marker for astrocytes: Comparing the distribution and expression of three astrocytic markers in different mouse cerebral regions. *BioMed Res. Int.* **2019**, *2019*, 9605265. [[CrossRef](#)]
52. Savchenko, V.; McKanna, J.; Nikonenko, I.; Skibo, G. Microglia and astrocytes in the adult rat brain: Comparative immunocytochemical analysis demonstrates the efficacy of lipocortin 1 immunoreactivity. *Neuroscience* **2000**, *96*, 195–203. [[CrossRef](#)] [[PubMed](#)]
53. Foust, K.D.; Nurre, E.; Montgomery, C.L.; Hernandez, A.; Chan, C.M.; Kaspar, B.K. Intravascular AAV9 preferentially targets neonatal neurons and adult astrocytes. *Nat. Biotechnol.* **2009**, *27*, 59–65. [[CrossRef](#)] [[PubMed](#)]
54. Mathiesen, S.N.; Lock, J.L.; Schoderboeck, L.; Abraham, W.C.; Hughes, S.M. CNS Transduction Benefits of AAV-PHP.eB over AAV9 Are Dependent on Administration Route and Mouse Strain. *Mol. Ther.-Methods Clin. Dev.* **2020**, *19*, 447–458. [[CrossRef](#)] [[PubMed](#)]
55. Maddalena, A.; Tereshchenko, J.; Bähr, M.; Kügler, S. Adeno-associated virus-mediated, mifepristone-regulated transgene expression in the brain. *Mol. Ther.-Nucleic Acids* **2013**, *2*, e106. [[CrossRef](#)] [[PubMed](#)]
56. Taschenberger, G.; Tereshchenko, J.; Kügler, S. A microRNA124 target sequence restores astrocyte specificity of gfaABC1D-driven transgene expression in AAV-mediated gene transfer. *Mol. Ther.-Nucleic Acids* **2017**, *8*, 13–25. [[CrossRef](#)]
57. Bushong, E.A.; Martone, M.E.; Jones, Y.Z.; Ellisman, M.H. Protoplasmic astrocytes in CA1 stratum radiatum occupy separate anatomical domains. *J. Neurosci.* **2002**, *22*, 183–192. [[CrossRef](#)]
58. Clavreul, S.; Abdeladim, L.; Hernández-Garzón, E.; Niculescu, D.; Durand, J.; Ieng, S.-H.; Barry, R.; Bonvento, G.; Beaurepaire, E.; Livet, J.; et al. Cortical astrocytes develop in a plastic manner at both clonal and cellular levels. *Nat. Commun.* **2019**, *10*, 4884. [[CrossRef](#)] [[PubMed](#)]
59. Theofilas, P.; Brar, S.; Stewart, K.-A.; Shen, H.-Y.; Sandau, U.S.; Poulsen, D.; Boison, D. Adenosine kinase as a target for therapeutic antisense strategies in epilepsy. *Epilepsia* **2011**, *52*, 589–601. [[CrossRef](#)]
60. Emsley, J.G.; Macklis, J.D. Astroglial heterogeneity closely reflects the neuronal-defined anatomy of the adult murine CNS. *Neuron Glia Biol.* **2006**, *2*, 175–186. [[CrossRef](#)] [[PubMed](#)]

61. Kimelberg, H. Astrocyte heterogeneity or homogeneity. In *Astrocytes in (Patho) Physiology of the Nervous System*; Haydon, P.G., Parpura, V., Eds.; Springer: New York, NY, USA, 2009; pp. 1–25. [[CrossRef](#)]
62. Matyash, V.; Kettenmann, H. Heterogeneity in astrocyte morphology and physiology. *Brain Res. Rev.* **2010**, *63*, 2–10. [[CrossRef](#)]

Disclaimer/Publisher's Note: The statements, opinions and data contained in all publications are solely those of the individual author(s) and contributor(s) and not of MDPI and/or the editor(s). MDPI and/or the editor(s) disclaim responsibility for any injury to people or property resulting from any ideas, methods, instructions or products referred to in the content.